5-2016

Non-Directional Conjugation of Fluorescent Antibodies to Gold Nanoparticles for Stem Cell Therapy

Kunal B. Shah
University of Arkansas, Fayetteville

Non-directional Conjugation of Fluorescent Antibodies to Gold Nanoparticles for Stem Cell Therapy

A thesis submitted in partial fulfillment
of the requirements for the degree of
Bachelors of Science in Biomedical Engineering

by

Kunal Shah

May 2016
University of Arkansas

Dr. Hanna Jensen
Thesis Director

PRIYA PUVANAKRISHNAN
Committee Member

Timothy J. Muldoon
Committee Member

MORTEN JENSEN
Committee Member / THESIS DIRECTOR

Committee Member

TABLE OF CONTENTS

Abstract

The objective of this study was to design citrate-coated gold nanoparticles conjugated with FITC-IgG, a fluorescent antibody, and to qualitatively and quantitatively measure the resulting fluorescent emission. Optical properties of the gold nanoparticles were measured at various stages to provide evidence of successful conjugation. The absorbance spectrum of the citrate gold nanoparticles was compared to that of the reaction mixture containing the gold nanoparticles and the FITC-IgG. A noticeable broadening of the absorption peak was observed at 519 nm indicating a surface modification of the gold nanoparticles. Fluorescence data was obtained with a fluorospectrometer and revealed a significant amount of fluorescent quenching in the reaction mixture as well as the washed mixture containing only fully conjugated molecules. However, the conjugated nanoparticles still emitted fluorescence at 519 nm as shown by the images captured under confocal microscopy. Based on the obtained optical densities of the reaction mixture and the FITC-IgG, the mass of molecules that were conjugated to the nanoparticles was calculated and determined to be approximately 24 FITC-IgG molecules per gold nanoparticle.

Introduction

Nanotechnology is an applied science involving particles on the scale of 1-100 nm in diameter. Advancements in the field of nanotechnology have proven to be applicable in the fields of computer engineering, physics, and of particular interest medicine. In 2007, nearly $60 billion worth of nanotechnology-based products were sold[3]. Currently in 2016, these figures have exceeded $1 trillion. However, at this stage nanotechnology is still in its infancy as its potential exceeds its products.

Nanomedicine has become one of the main fields of research involving nanotechnology. It has the potential to develop new methods of diagnosing, preventing and treating various diseases. Many of these applications stem from the fact that nanoparticles such as those made of silver (Ag) and gold (Au) are unique due to their size on the nanoscale. Electrons in the conduction band tend to oscillate at some extinction peak when light of a wavelength comparable in size to the nanoparticle is incident as shown in Figure 1. This is called localized surface plasmon resonance (LSPR). As a result of the LSPR phenomenon, a resonant field surrounds the nanoparticle getting stronger as the distance from the surface decreases. Thus, being smaller than the wavelength of light allows nanoparticles to exhibit unique physical and optical properties.[4]

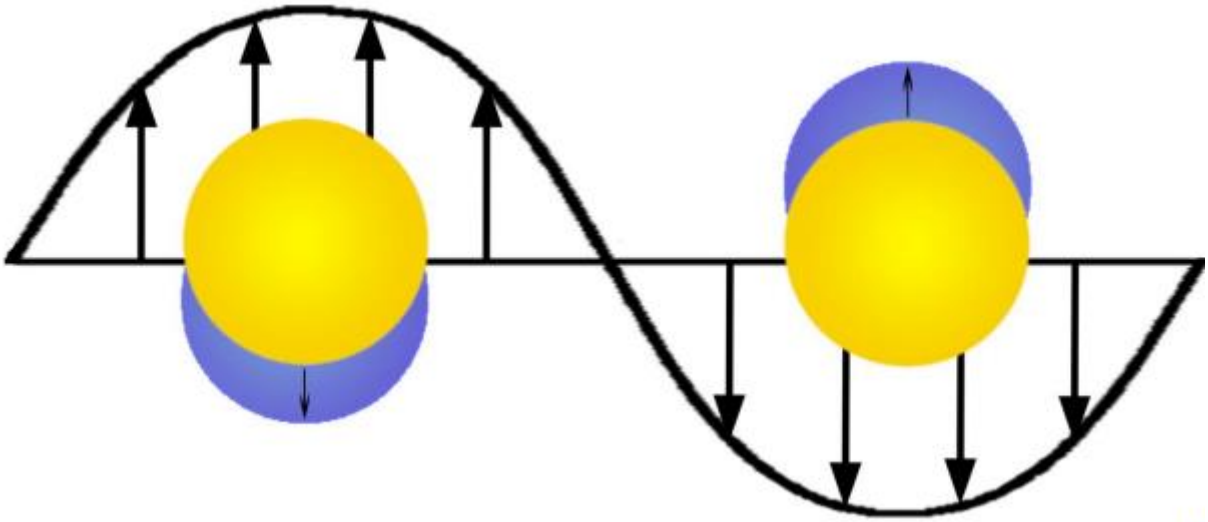

Figure 1: Localized surface plasmon produced by interaction between the free electrons in the particles and an incident electromagnetic wave. [9]

Gold nanoparticles have several properties that make them promising agents for stem cell labeling and tracking. They are easy to manufacture and conjugate to a wide variety of biomolecular targets[5]. Furthermore, *In vitro* studies have shown that mesenchymal and adipose-derived stem cells labeled with gold nanoparticles did not demonstrate changes in cell function or proliferation, and no toxicity was apparent. The binding of gold nanoparticles to stem cells requires the expression of an antibody specific to a protein that is characterized on the surface of the stem cell of interest. This can be accomplished by conjugating antibodies to gold

nanoparticles through various binding mechanism. The nanoparticle is first coated with citrate, a stabilizing agent. This negatively charged coating prevents the nanoparticles from aggregating in solution. The first binding mechanism is via hydrophobic interactions. Hydrophobic parts of the antibodies become attracted to the surface of the nanoparticle forming a non-covalent bond. The second binding mechanism is through electrostatic interactions of positively charged amino acids on the antibodies and the negatively charged citrate coating. The last mechanism is through covalent bonds between the nanoparticle and free sulfhydryl groups of the antibody. As a result, controlling the directionality of the antibodies would require new conditions for binding. The mechanisms described are shown respectively in the schematic in Figure 2[11].

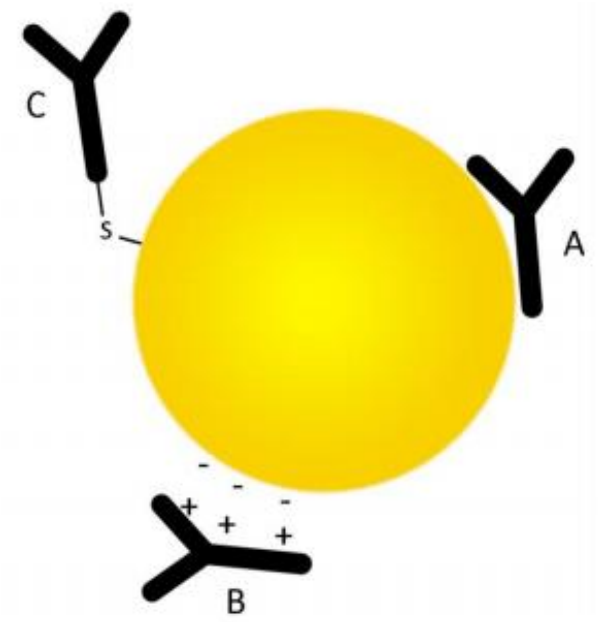

Figure 2. A Schematic diagram of possible orientations of antibodies on AuNPs.

Once bound, nanoparticles can be further engineered for potential use as a stem cell delivery system to areas of the body that require cell/tissue regeneration. One such application is in the regeneration of ischemic cardiac tissue after an acute myocardial infarction (AMI). In the United States, cardiovascular disease is the leading cause of death in the United Sates, claiming more lives than all forms of cancer combined[1]. Of the various forms of heart disease, coronary artery disease (CAD) is the most common, eventually leading to AMI. Every year approximately 735,000 Americans suffer from AMI[1]. Atherosclerosis, the buildup of plaque (fat, cholesterol, and other substances) in the coronary arteries, causes the blood vessels to narrow and ultimately restricts the flow of blood to the myocardium.

As blood flow is interrupted in an AMI, cardiomyocytes begin to die because they are unable to obtain oxygen and the necessary nutrients for survival. This condition is known as myocardial ischemia. If the adequate blood is not quickly restored, the surrounding cardiac tissue undergoes apoptosis or necrosis. Human cardiomyocytes have a very limited ability to

regenerate, thus as the heart begins to remodel after ischemia, the cardiac muscle tissue is irreversibly replaced by fibrotic collagen scar tissue. The scar tissue therefore disrupts proper contractile function resulting in decreased cardiac performance, ventricular dilation, and wall thinning. This process of remodeling continues until the fibrotic scar's tensile strength balances the distending forces of the heart[3]. The ischemic tissue lacks function during systole, therefore unable to contract of contribute to pressure generation associated with the heart. This forces other anatomical segments of the heart to overcompensate leading to chronic ischemic cardiomyopathy and congestive heart failure. Stem cell therapies have been extensively researched in order to promote regeneration of cardiac tissue, but have several challenges such as cell homing, retention and appropriate differentiation to cardiac muscle. Nanotechnology is a novel approach that may assist in the delivery and tissue retention of stem cells. Despite significant advances in the clinical treatment and prevention of AMI, this sort of nanotechnology-based stem cell therapy has not yet been performed *in vivo* and over 370,000 Americans still die from CAD each year[2].

Before nanotechnology is used i*n vivo*, there is a need to address issues like opsonization, phagocytosis by macrophages, and sequestration to the liver and spleen for eventual elimination from the body[6]. Information in this regard would help to determine the gold nanoparticle's longevity in circulation and clearance rate from the body. The fates of these nanoparticles depend heavily on their physio-biochemical properties, including their size, shape, and surface chemistry. Novel approaches have reported to alter the surface chemistry of nanoparticles to obtain desirable functionality allowing for greater blood circulation times as well as increased biocompatibility[7].

Since the functionality of nanoparticles *in vivo* is still under scrutiny, tagging conjugated gold nanoparticles with a fluorophore can allow researchers to locate and image these particles under ultra violet (UV) light. The fluorophore used in this study, FITC has an excitation maximum at 490 nm and an emission maximum at 525 nm with a high quantum yield of 0.93[10]. The quantum yield of a fluorophore is the number of photons emitted per photon absorbed. In other words it is a measure of efficiency 0.0 being completely inefficient and 1.0 being maximally efficient. Greater quantum yields are more desirable as they are stronger fluorescents and are easier to image using fluorescent imaging techniques.

The objective of this study is to conjugate citrate gold nanoparticles with a fluorescent antibody, FITC-IgG, and show successful conjugation and fluorescence. Successful completion of this will allow further applications of stem cell therapy for treatment of myocardial infarctions through nanotechnology.

Materials and Methods

Preparation of Citrate Au Nanoparticles:

15 nm diameter Au particles were prepared by citrate reduction of HAuCl4. Images were then captured using a Transmission electron microscope (TEM) to observe the nanoparticles and determine the size and dispersity. TEM image is shown in Figure 3.

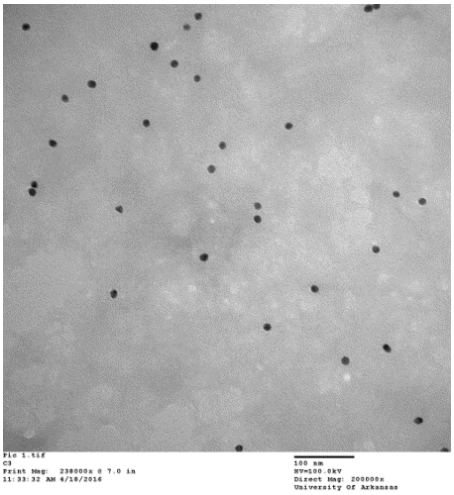

Figure 3 TEM image of citrate Au nanoparticles.

A spectrophotometer was used to measure the absorbance of the gold nanoparticles are various wavelengths to confirm particle identity. 1mL of the citrate gold solution (0.1mg/mL) was centrifuged at 11,000 revolutions per minute (RPM) for 15 minutes. The supernatant was removed and 100 µL of K-PBS was added. This tube was labeled A. The optical density was obtained of tube A. The absorbance spectrum is shown in Figure 4.

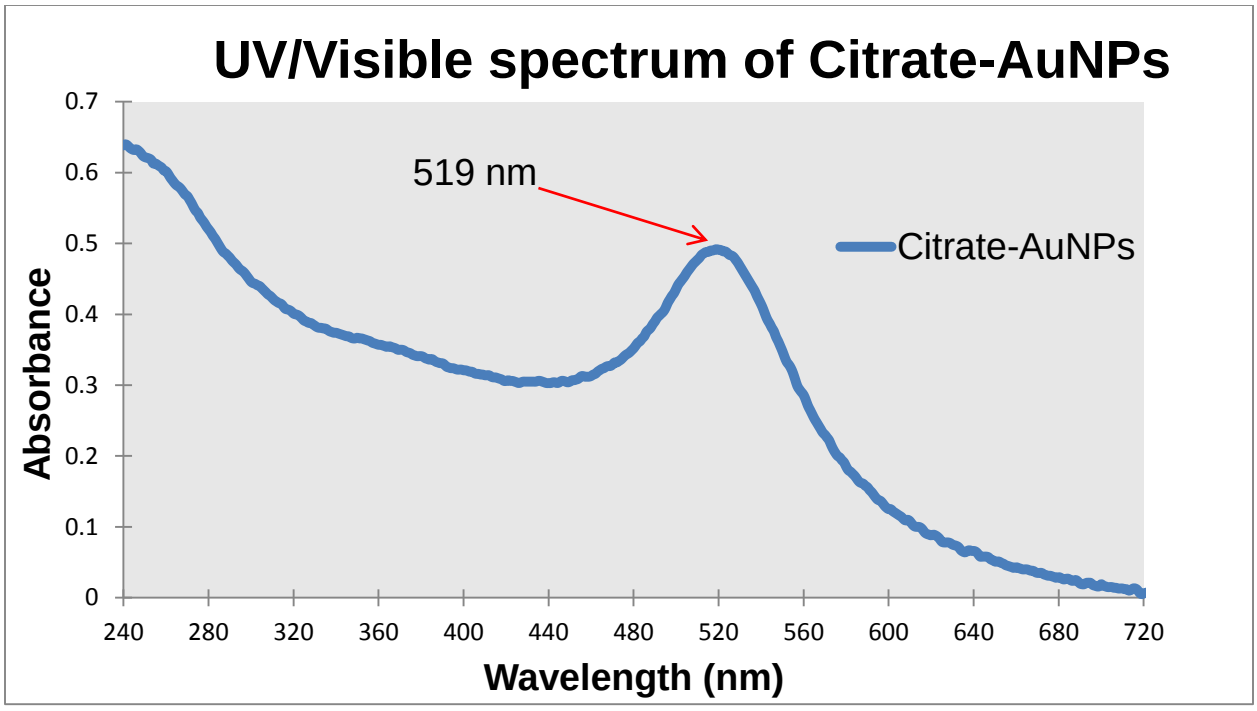

Figure 4. The absorbance spectrum of citrate gold nanoparticles shows an emission peak at 519nm.

Conjugation of Au Nanoparticles with FITC-IgG:

40 µL of FITC-IgG was added to 60 µL of K-PBS and was labeled B. The absorbance spectrum of tube B was obtained and images of tube B under UV light was captured. The fluorescence of tube A and tube B were measured with the fluorospectrometer and is shown in Figure 7. The 1 mL contents of tube B was added dropwise into tube A while it was vortexed. This solution contained both the Au nanoparticles and the FITC-IgG molecules and was labeled tube C. The mixture was incubated at room temperature without shaking for 10 minutes. The contents of tube C were placed in the fluorospectrometer to obtain its fluorescence spectra. Images of tube C were taken next to tube A under UV light.

Washing of Unreacted Molecules:

The mixture was then centrifuged at 11,000 RPM for 15 minutes. The supernatant was then removed and the optical density of the supernatant solution was measured using the spectrophotometer. 1 mL of potassium phosphate-buffered saline (K-PBS) containing bovine serum albumin (BSA) was added and mixed. This mixture was centrifuged at 11,000 RPM for 15 minutes and the supernatant was removed. Another 1 mL of K-PBS containing BSA was added and then centrifuged at 11,000 RPM for 15 minutes removing the resulting supernatant. 200 µL of K-PBS (pH 8.2, 2mM) was added to the tube and mixed. The optical density and fluorescence of this resulting solution was measured.

Calculations

The optical density of the supernatant unreacted mixture of FITC-IgG and AuNPs was measured and subtracted from the optical density of FITC-IgG alone.

$$0.624 - 0.227 = 0.397$$

This gives the optical density of bound FITC-IgG molecules which proportionally corresponds to a mass. The mass of FITC-IgG alone was 0.06mg. So the mass of bound FITC-IgG is proportional based on the absorbance.

$$\frac{0.624}{0.397} = \frac{0.06\ mg}{x}$$

x = 0.03817 mg bound FITC-IgG

The mass can be converted to a number of moles using the molecular weight of IgG, 150 kg.

$$\frac{0.03817\ mg}{1} * \frac{1\ g}{1000\ mg} * \frac{1\ kg}{1000\ g} \frac{1\ mol\ IgG}{150\ kg} = 2.5467 * 10^{-10}\ mol\ IgG$$

The number of moles can then be converted to a number of particles using Avogadro's number.

$$\frac{2.5467 * 10^{-10}\ mol\ IgG}{1} * \frac{6.023 * 10^{23}\ particles}{1\ mol} = 1.5339 * 10^{14}\ IgG\ particles$$

The ratio of FITC-IgG particles to the number of AuNPs particles in solution, gives an approximation of FITC-IgG molecules bound per nanoparticle.

$$\frac{1.5339 * 10^{14}\ IgG\ particles}{6.37 *\ 10^{12}\ AuNPs} \approx \mathbf{24\ IgG\ molecules\ bound\ per\ AuNP}$$

There are approximately 24 FITC-IgG molecules bound per AuNP.

Results

The absorbance spectrum of the citrate-AuNPs was compared to the FITC-IgG conjugated citrate-AuNPs and is shown in Figure 5. A noticeable red-shift was detected once the antibodies were bound to the nanoparticles. There was also a slight broadening of the extinction peak.

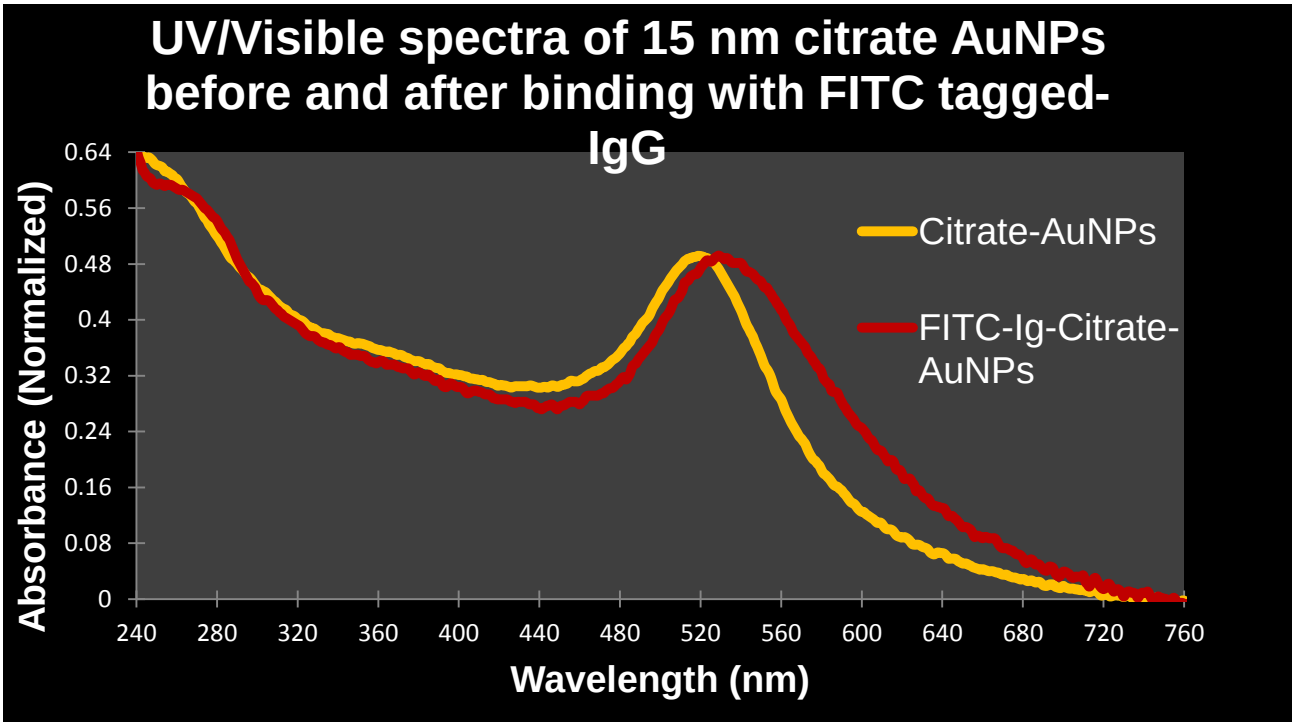

Figure 5 Spectrophotometer: After FITC-IgG conjugation of AuNPs, a slight red-shift was observed and a noticeable broadening of the absorbance peak. This is an indication of successful conjugation. Absorbance increased at 280nm indicating the presence of proteins.

In addition, the line for the conjugated AuNPs showed an absorbance peak at 280 nm, which is the same wavelength at which proteins have peak absorbance[15].

Images of FITC-IgG, unwashed conjugated AuNPs, and washed conjugated AuNPs were captured under UV light and were compared in Figure 6. Image A, showed a very strong fluorescence. Image B still showed a strong fluorescence but quenched. After washing away unreacted molecules from the tube from image B the fluorescence was further reduced.

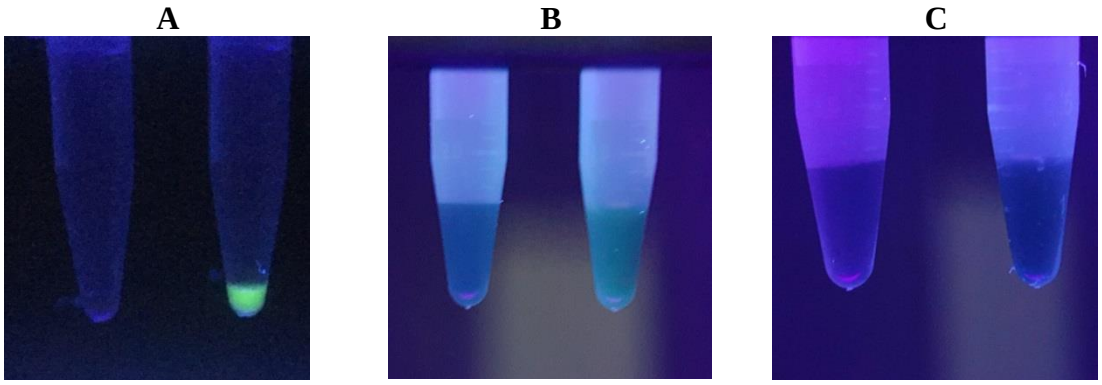

Figure 6 UV Light: Image A compares fluorescence of AuNPs to FITC-IgG. Image B compares AuNPs to FITC-IgG + AuNPs. Image C compares AuNPs to conjugated AuNPs.

A comparison of the relative fluorescence for the AuNPs, FITC-IgG, and the unwashed reaction mixture is shown in Figure 7. This data is consistent with the UV light images from Figure 6. Once the nanoparticles are mixed with the fluorescent antibodies, the magnitude of the fluorescence decreased almost six-fold.

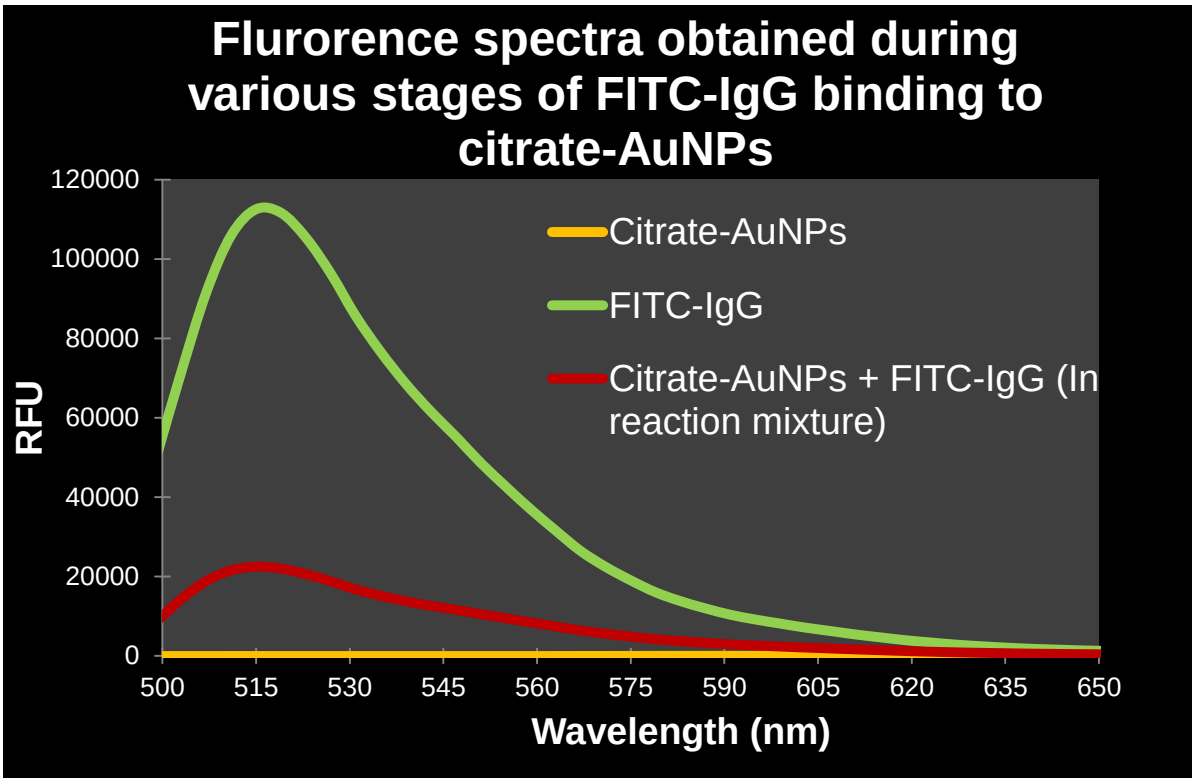

Figure 7 Fluorospectrometer: Relative fluorescence measurements were obtained for each substrate and product. Fluorescence was quenched for the reaction mixture.

After washing the mixture, the fluorescence spectrum in Figure 8 showed further quenching of the fluorescence. However, a fluorescence signal still exists.

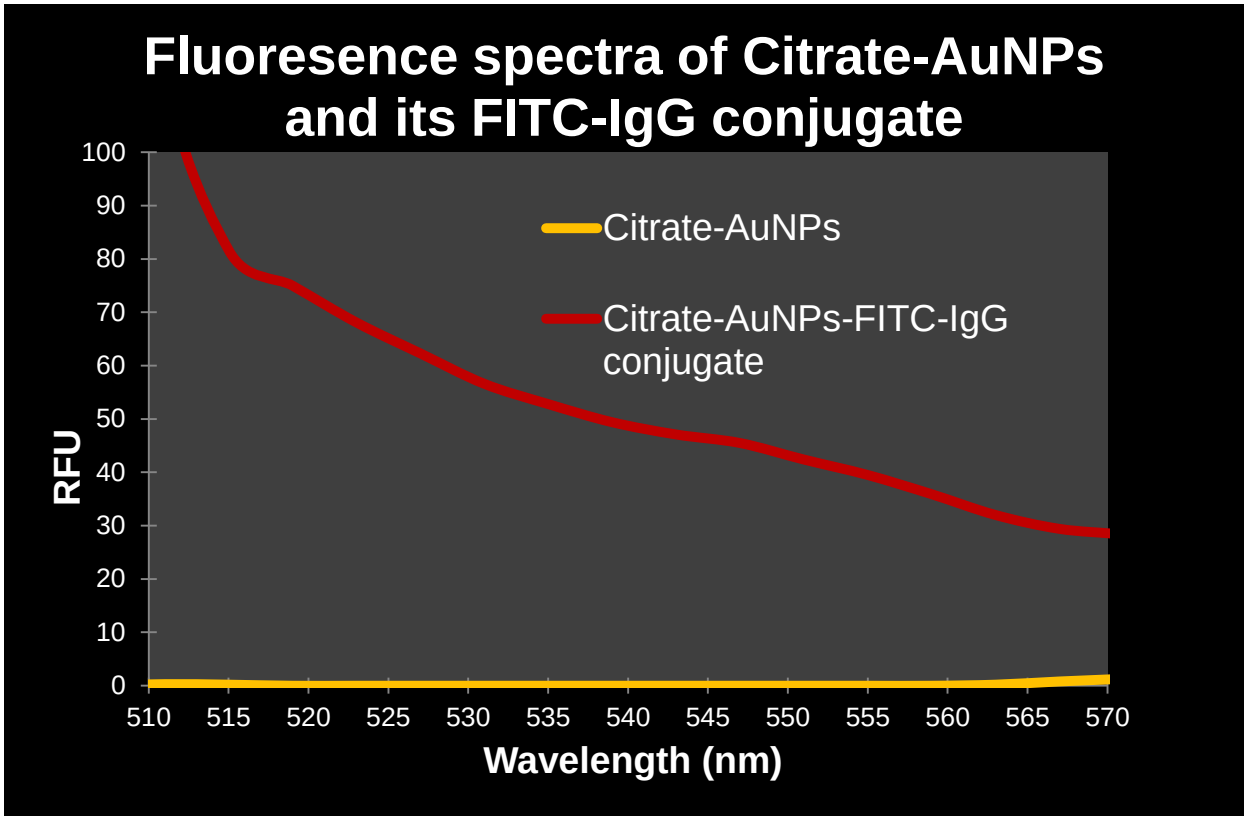

Figure 8 Fluorescence is further reduced after washing unreacted molecules

The BIO-RAD Gel Doc system was used to conduct a fluorescence test comparing the signal from the citrate-AuNPs mixture and the conjugated FITC-IgG AuNPs. Figure 9 below compares the image of the slide before and after placing it into the Gel Doc system. A signal containing no fluorescence will show no color and a signal containing fluorescence will show up white. The images in Figure 9 outline a faint fluorescent signal from the conjugated nanoparticle. This information is consistent with the fluorospectrometer readings.

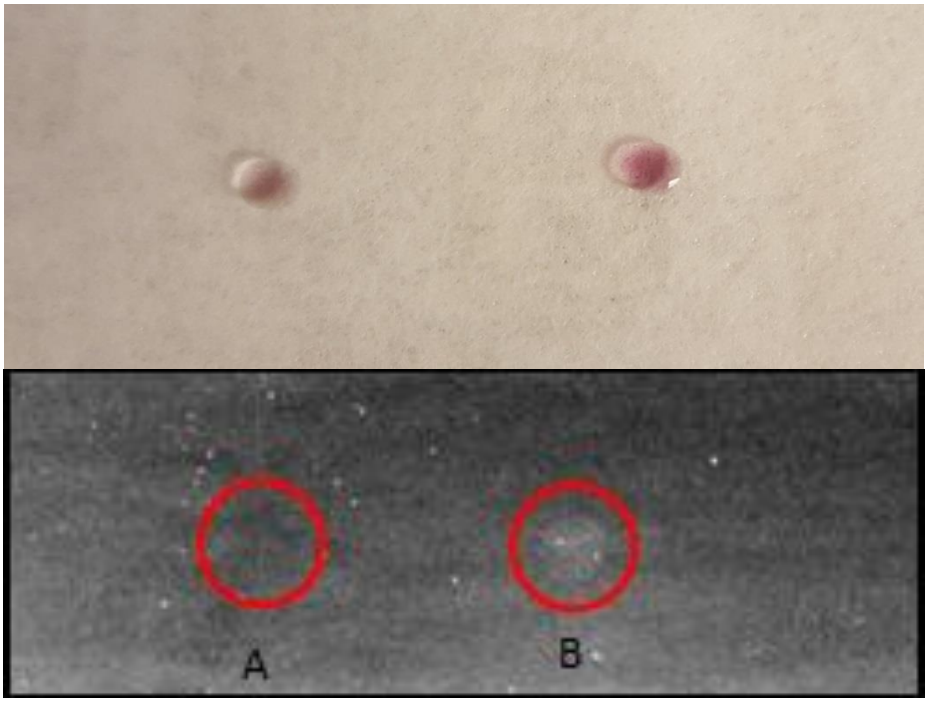

Figure 9 Dot Test: Using the BIO-RAD Gel Doc system, a fluorescent detection test was conducted to further investigate fluorescent properties of the conjugated AuNPs. (A) Citrate AuNPs control, (B) Conjugated AuNPs.

To complete our data acquisition, images were taken using a Leica Confocal Microscope SP5II. The advantage of using a laser scanning confocal microscope is reduced blurriness of images due to light scattering, increased resolution and an improved signal-to-noise ratio through the use of a pinhole at the confocal plane of the lens that serves to eliminate out of focus light[16]. For the image shown in Figure 10 four laser wavelengths were used for excitation at a power level of approximately 5%; 488 nm, 496 nm, 514 nm, 633 nm. The maximum emission wavelength range for FITC is 520 nm to 530 nm[12]. The confocal images showed a significant number of small particles that fluoresced with some being larger and stronger than others.

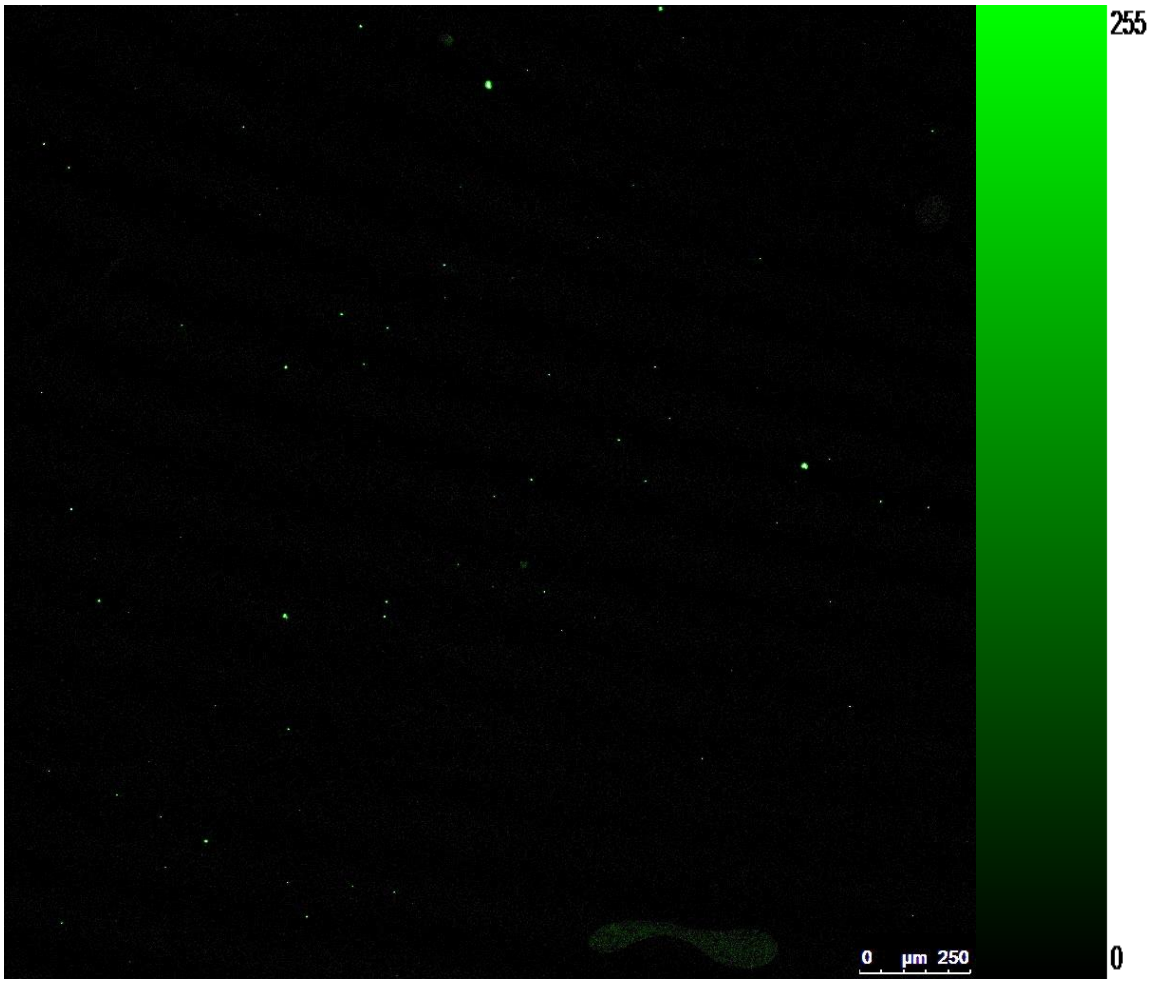

Figure 10 Confocal Microscopy: The confocal image of the final conjugated product indisputably revealed several fluorescent nanoparticles to conclude the investigation.

Discussion & Future Directions

The spectrophotometer readings in Figure 5 were an indication of molecule adsorption to the surface of the AuNPs due to a change in refractive index of the surrounding solution[9]. There was also a slight broadening of the extinction peak which occurs with particles of greater size. Since proteins generally have the greatest absorbance at 280 nm, we can conclude that the conjugated particles contained antibodies. The fluorospectrometer readings in Figure 7 showed us that the addition of the fluorescent antibodies to the AuNPs solution is reducing the fluorescence to one that is in between that of the two individual components. Furthermore, assuming all unreacted FITC-IgG molecules were removed, the signal of the unwashed mixture from Figure 8 may have been from the free flowing FITC-IgG. Thus, the washed mixture showed a signal characteristic of the conjugated nanoparticles only. This must mean that the sole binding of the FITC-IgG to the AuNPs is resulting in a quenched fluorescence of the

fluorophore.It may be possible that unreacted FITC-IgG molecules remained in solution after being washed. We would expect these molecules to fluoresce equally. The confocal microscope image in Figure 10 shows some stronger than others which may allow us to be certain to some degree that the lower intensity fluorescent particles are those that are conjugated to the gold nanoparticles and thus quenched.

The spectrophotometer readings were strong indications that conjugation of gold nanoparticles with the fluorescent antibodies was successful. However, a significant amount of quenching of the fluorescence was evident from the various fluorescence detection tests. Fluorescence can be quenched due to the nanoparticle's plasmon field strength. As the distance of the fluorescent agent increases from the nanoparticle's surface, the field strength decreases and the effects of quenching are significantly reduced[13]. To combat this issue a linker molecule could be used to extend the fluorescent antibody away from the nanoparticle. This would allow for the plasmon field strength to have a lesser electronic impact on the quenching of the fluorescence. Other studies have suggested that having the nanoparticle's absorbance peak in the same region as the fluorophore's emission peak could impact the ability for the fluorophore to be fully expressed.

In this particular study, the directionality of the antibodies was not controlled; therefore further imaging is required to confirm that the constant region was bound directly to the nanoparticles[14]. For stem cell therapy to applicable the variable region to the antibody must be exposed to attract and bind specific antigens. In addition, controlling the directionality of the bound antibodies will allow scientists to predict how close the fluorophore is to the nanoparticle surface and thus predicting the amount of fluorescent quenching.

The mechanisms used in this study involved non-covalent binding. Other methods of binding could be employed for increased stability and directional orientation such as covalent bonds involving free sulfhydryl groups[14].

In conclusion, gold nanoparticles were successfully conjugated with fluorescent antibodies, and the methodology for a subsequent stem cell study was developed and validated. The ease of detection of nanoparticles is extremely important as we consider an in vivo study, and thus quenching must be minimized. Prior to proceeding to experiments with stem cells, we plan to test the utilization of a linker molecule, control the directionality of the antibodies, and explore covalent bonding to improve nanoparticle fluorescence.

Acknowledgements

I would like to thank both of my honor's research advisors Dr. Hanna Jensen and Dr. Morten Jensen for everything they have done to make sure I completed this project on a timely manner while also making sure I met all the standards. Thanks to Dr. Arvind Sinha for teaching me the proper lab techniques and mentoring me through the protocol. Many thanks to Dr. Elizabeth Martin for helping capture images with the confocal microscope and Dr. Jin-Woo Kim for helping create the protocol and providing the materials and lab space.

References

1. Mozaffarian D, Benjamin EJ, Go AS, et al. Heart disease and stroke statistics—2015 update: a report from the American Heart Association. *Circulation*. 2015;131:e29-322.
2. CDC, NCHS. Underlying Cause of Death 1999-2013 on CDC WONDER Online Database, released 2015. Data are from the Multiple Cause of Death Files, 1999-2013, as compiled from data provided by the 57 vital statistics jurisdictions through the Vital Statistics Cooperative Program. Accessed Feb. 3, 2015.
3. "Introduction to Nanotechnology." Projects on Emerging Nanotechnologies. 2008. Accessed April 26, 2016. Processwire.
4. Hao, F., Sonnefraud, Y., Dorpe, P. V., Maier, S. A., Halas, N. J., & Nordlander, P. (2008). Symmetry breaking in plasmonic nanocavities: subradiant LSPR sensing and a tunable Fano resonance. Nano letters, 8(11), 3983-3988.
5. Accomasso L, Gallina C, Turinetto V, Giachino C. Stem Cell Tracking with Nanoparticles for Regenerative Medicine Purposes: An Overview. Stem Cells Int. 2016;2016:7920358
6. Ricles LM, Nam SY, Sokolov K, Emelianov SY, Suggs LJ. Function of mesenchymal stem cells following loading of gold nanotracers. International Journal of Nanomedicine. 2011;6:407-16.
7. Kim JW, Galanzha EI, Zaharoff DA, Griffin RJ, Zharov VP. Nanotheranostics of circulating tumor cells, infections and other pathological features in vivo. Molecular pharmaceutics. 2013;10(3):813-30.
8. Willets, K., van Duyne, R. Localized Surface Plasmon Resonance Spectroscopy and Sensing. Annual Review Physical Chemistry. 2007, 58, pp. 267-297.
9. Willets, K., van Duyne, R. Localized Surface Plasmon Resonance Spectroscopy and Sensing. Annual Review Physical Chemistry. 2007, 58, pp. 267-297.
10. Sjöback, Robert, Jan Nygren, and Mikael Kubista. "Absorption and fluorescence properties of fluorescein." *Spectrochimica Acta Part A: Molecular and Biomolecular Spectroscopy* 51, no. 6 (1995): L7-L21.
11. Hermanson, G. Bioconjugate Techniques 2nd ed. San Diego : Academic Press, 2008.
12. Ma, Qiang, Xinyan Wang, Yabing Li, Yuhua Shi, and Xingguang Su. "Multicolor quantum dot-encoded microspheres for the detection of biomolecules." Talanta 72, no. 4 (2007): 1446-1452.
13. Dulkeith, E., A. C. Morteani, T. Niedereichholz, T. A. Klar, J. Feldmann, S. A. Levi, F. C. J. M. Van Veggel, D. N. Reinhoudt, M. Möller, and D. I. Gittins. "Fluorescence quenching of dye molecules near gold nanoparticles: radiative and nonradiative effects." Physical review letters 89, no. 20 (2002): 203002.
14. Ljungblad, Jonas. "Antibody-conjugated gold nanoparticles integrated in a fluorescence based biochip." (2009).
15. Whitaker, John R., and Per Einar Granum. "An absolute method for protein determination based on difference in absorbance at 235 and 280 nm." Analytical biochemistry 109, no. 1 (1980): 156-159.

16. Gmitro, Arthur F., and David Aziz. "Confocal microscopy through a fiber-optic imaging bundle." Optics letters 18, no. 8 (1993): 565-567.